Experimental study on ultimate torsional strength of PC composite box-girder with corrugated steel webs under pure torsion

Yong Ding[*1], Kebin Jiang[1a], Fei Shao[1b] and Anzhong Deng[2c]

[1]*Department of Bridge and Tunnel Engineering, PLA University of Science and Technology, No.1 Haifu Lane, Baixia District, Nanjing City, China*
[2]*Department of Civil Engineering, Institute of Logistics Engineering of PLA, Chongqing Municipality, China*

Abstract. To have a better understanding of the torsional mechanism and influencing factors of PC composite box-girder with corrugated steel webs, ultimate torsional strength of four specimens under pure torsion were analyzed with Model Test Method. Monotonic pure torsion acts on specimens by eccentric concentrated loading. The experimental results show that cracks form at an angle of 45° to the member's longitudinal axis in the top and bottom concrete slabs. Longitudinal reinforcement located in the center of cross section contributes little to torsional capacity of the specimens. Torsional rigidity is proportional to shape parameter η of corrugation and there is an increase in yielding torque and ultimate torque of specimens as the thickness of corrugated steel webs increases.

Keywords: corrugated steel webs; composite box girder; ultimate torsional strength; cracks; space truss

1. Introduction

As a result of the replacement of traditional concrete webs by corrugated steel ones, PC composite box-girder with corrugated steel webs (CBCSWs) has been a completely new kind of hybrid structure with the merits of light weight, high shear strength of webs and good efficiency of prestressing (Cheyrezy and Combault 1990, Metwally and Loov 2003). Since the first prestressed concrete box-girder bridge with corrugated steel webs was built in France in 1986 (Combault 1988), the performance of this type of box-girder has been studied worldwide.

The flexural behavior of the structure as a whole was studied experimentally and numerically by Elgaaly *et al.* (Elgaaly *et al.* 1997, Elgaaly and Seshadri 1998). Moon and Yi conducted studies on shear behavior of corrugated steel webs (Moon *et al.* 2009, Yi *et al.* 2008). Besides these researches, there are also large quantities of articles discussing the shear response and flexural behavior of this structure (Elgaaly and Hamilton 1996, Song *et al.* 2004, Jiang *et al.* 2011, Chuslip

---

*Corresponding author, Ph.D. Student, E-mail: pla_yong@163.com
[a]Professor, E-mail: kbjiang@sina.com
[b]Ph.D., E-mail: shaofeiriver@163.com
[c]Ph.D., E-mail: denglin929@126.com

and Usami 2002, Robert *et al.* 2006). Torsional strength of RC beams was studied by Cevik *et al.* (2012), but little work about the torsional behavior of PC box-girder with corrugated steel webs has been reported. Mo *et al.* (2000) conducted experimental and analytical studies for four scaled PC CBCSWs subjected to cyclic torsion. A three dimensional finite element model of PC CBCSWs was established by Ding *et al.* (2012) and a parametric study was carried out. There is still dearth of experimental data of PC CBCSWs subjected to torsion.

To have a better understanding of the torsional mechanism and influencing factors of PC CBCSWs and to provide more documents, four scaled specimens have been tested in this paper. Ultimate torsional strength of these specimens under pure torsion is obtained and experimental phenomena and results are presented in details.

2. Research significance

The development of calculation theory and computer technology makes the refinement of the design for civil engineering structures possible. Almost all of current design codes (CEN 2005, AISC 2005, JTG D62-2004) adopt limit state method based on probabilistic concepts of safety, which requires more understanding of ultimate bearing capacity of structures. The torsional rigidity of PC CBCSWs is reduced compared to that of traditional concrete box-girder. Experimental Method is a relatively accurate and effective solution to obtain ultimate bearing capacity of structures among the available methods.

3. Experimental program

3.1 Specimens

The model test consists of four specimens with the same section dimension of 0.64×0.45mm as shown in Fig. 1(a). Four specimens are designated as PT-1, PT-2, PT-3 and PT-4 respectively. There are end diaphragms of 0.2m thickness at both ends of each specimen. Characters PT stand for pure torsion while character 1 to 4 denotes the number of specimen. Two types ofcorrugation shape are designed to investigate their effect on torsional behavior, and meanwhile the influence of steel web thickness is studied including t_w = 2, 2.8 and 3mm, in which *tw* is thickness of steel webs. To transfer shear forces from steel web to concrete slab, the corrugated steel webs areperforated with ϕ20mm holes along longitudinal direction, through which ϕ10mm stirrups go. Fig. 1(b) shows a schematic diagram where this type of connection is applied to a composite box girderwith corrugated steel webs. All parameters of PT-2 are the same with those of PT-1 except a steel bar arranged in the middle of the section (as shown in Fig. 1(a)) which is used to learn the stress state of steel bars located outside the shear flow zone. Specific parameters of specimens are listed in Table 1.

3.2 Material properties

Portland cement was used in all of the concrete mixtures. Crushed gravel was used as the coarse aggregate, where in the maximum aggregate size, G_{max}, was 25 mm as shown in Table 2.

Table 1 Geometric and material parameters of specimens

Specimens	$f_c'^*$ (MPa)	σ_y (MPa)			F_p (kN)	t_w (mm)	Corrugation shape	η^*
		long. reinf.	stirrup	steel web				
PT-1	33.1	335	335	292	100	3	CI	0.909
PT-2	35.8	335	335	292	100	3	CI	0.909
PT-3	32.8	335	335	292	100	2.8	CII	0.920
PT-4	25.1	335	335	292	100	2	CI	0.909

*η is shape parameter of corrugated steel webs, $\eta = (a+b)/(a+c)$; f_c' is compressive strength of concrete cylinder, $f_c' = 0.76 f_{cu}'$
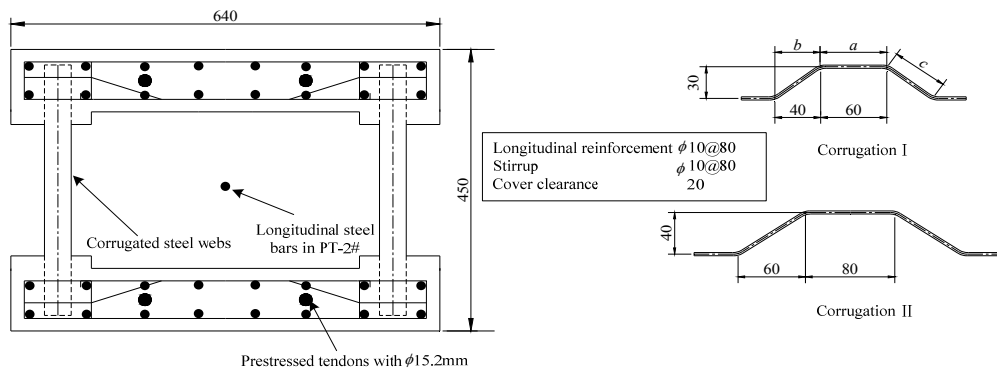
(a) Section dimension and corrugation shape
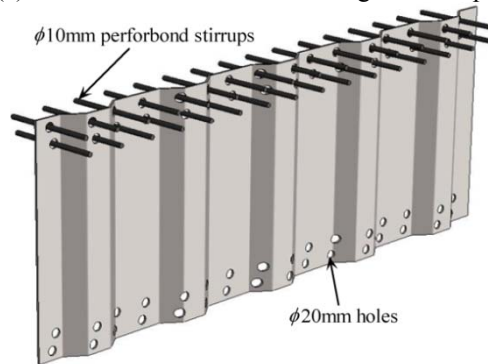
(b) Typical layout of perforbond stirrups
Fig. 1 Dimension and configuration of specimens (Unit:mm)

The compressive strength of concrete cubes, f_{cu}', was measured as the average of three identical cubes, each of which was a cube 150mm long. These cubes were tested under axial loading at the time when the corresponding specimen was tested. The steel plate used in the specimens with corrugated web was Q235, and the average yield strengths were 292MPa. 16-ϕ10 steel bars with the grade of HRB335 were placed in two layers with the spacings of 80 mm in the top and bottom slabs as longitudinal reinforcement. Seven wired low relaxation tendons with 15.2 mm diameters were used for all specimens and their ultimate tensile strength is 1860MPa.

Table 2 Concrete mix proportion

Material	Cement	Sand	Crushed gravel	Water	Admixture	Fly ash
Specification	P.O 42.5	Medium	5~25mm continuous grading	Drinking water	-	-
Mix proportion (kg/m^3)	425	850	1000	150	6.000	50

3.3 Fabrication

Fig. 2 presents the whole fabrication flow of all four specimens, of which the top and bottom slabs were casted separately. Reinforcement and prestressed tendons in the bottom slab were arranged first and highly flowable concrete was used as the concrete infilling. After pouring and vibrating of concrete as shown in Fig. 2(b), the concrete of the bottom slab was cured for one day before formworks of top slab were set. From Fig. 2(d), it can be seen that a wooden board and compacted sand were adopted to support concrete of the top slab because of the corrugation characteristic. The top slab was casted after the layout of reinforcement and prestressed tendons. Six concrete cubes were fabricated at the same time as the top slab was casted of each specimen and cured under the same condition of corresponding specimen. Three of these cubes were used to get the prestressing time while the other three were used to obtain the concrete strength of specimen under test. One day after concrete curing of top slab, the formworks were removed and end diaphragms were casted subsequently. The tendons were not prestressed until the concrete strength approached 90 percent of its design compressive strength. Fig. 2(h) and Fig. 2(i) show the ultimate form of two specimens denoted as PT-1 and PT-2, respectively.

(a) formwork and reinforcement of bottom slab   (c) curing concrete of bottom slab   (d) formwork of top slab   (e) reinforcement of top slab   (f) curing concrete of top slab

(h) PT-1#

(b) casting concrete of bottom slab   (g) prestressing tendons   (i) PT-2#

Fig. 2 Fabrication of a composite box girder with corrugated steel webs

Fig. 3 Test setup

(a) Side view

(b) Top view
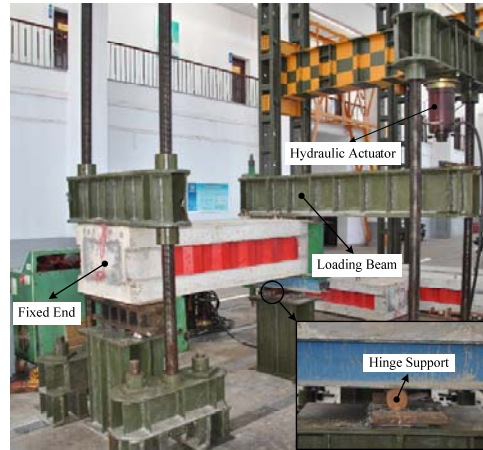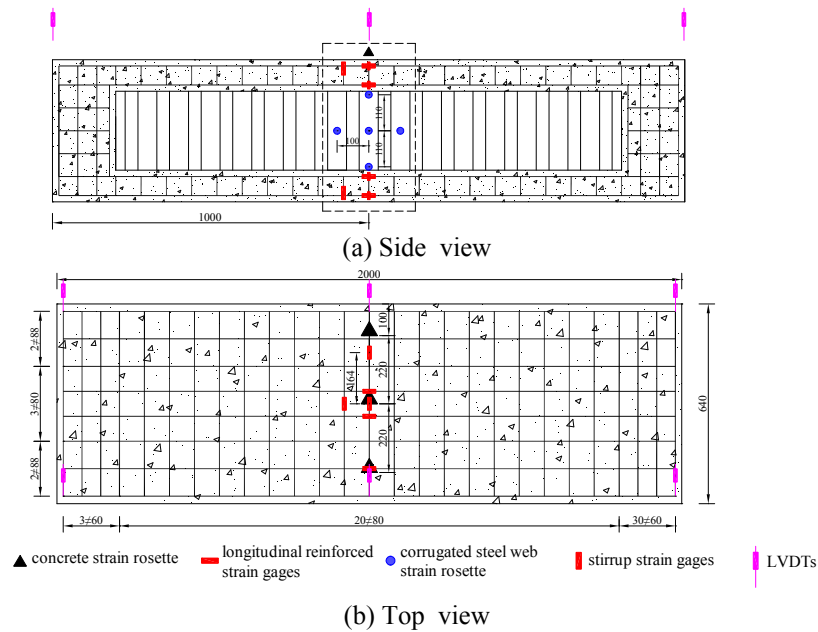Fig. 4 Arrangement of the measuring points(Units:mm)

3.4 Test setup and procedures

The test setup is shown in Fig. 3. The specimens were clamped at both ends by I-shaped steels. The clamping I-shaped steels were fastened by nuts and threaded rods. One end of the specimens was fixed. The specimen was held on a steel seat supported by the strong floor. The other end was a rotating one, and was subjected to torsion via a lever arm of 1.5m. Each specimen was instrumented with load cells, linear variable displacement transducers (LVDTs), and strain gages to monitor the applied displacement and corresponding loads as well as the resulting strains and relative deformations. Fig. 4 displays the location of LVDTs and strain gages. During the test, the

force-controlled procedures were used. The specimens were loaded following the prescribed steps with 25kN of each step before cracking and 10kN after cracking. The test continued until failure occurred, that is, the force dropped sharply.

4. Experimental results

4.1 General observation

The experimental phenomena of four specimens, which consist of three stages, are almost the same. Stage I: elastic phase, in which the external torque is counteracted by the whole composite section made up of the corrugated steel webs, the concrete top and bottom slabs. Deformation of longitudinal reinforcement, stirrup and concrete is compatible in this phase which ranges from the beginning of loading to initiation of cracks. Stage II: space truss phase, starting from the appearance of cracks. Primary diagonal cracks form in the top and bottom slabs and are inclined at an angle of approximately 45° to the specimen's longitudinal axis when the external torque reaches cracking torque. As the external torque increases, the number and width of cracks increases larger. The inclined angle of cracks is observed to be relatively uniform during the loading increment. Space truss is gradually formed in the top and bottom concrete slabs involving longitudinal reinforcement, stirrup and concrete strut and torsional rigidity of composite box girder decreases as the external torque increases. Stage III: yield and failure phase. If the load continues to increase after cracks fully develop, yield may occur in longitudinal reinforcement, stirrups or corrugated steel webs. Once yield occurs in the top or bottom concrete slabs, twist of the composite box girder will increase dramatically which results in the main cracks with the largest width to bring shear failure mode. On condition that there were thinner corrugated steel webs, yield would occur in webs prior to reinforcements or stirrups in the top and bottom concrete slabs. The loss of torsional bearing capacity of the composite box girder goes with the yield of reinforcements or stirrups, but not that of corrugated steel webs.
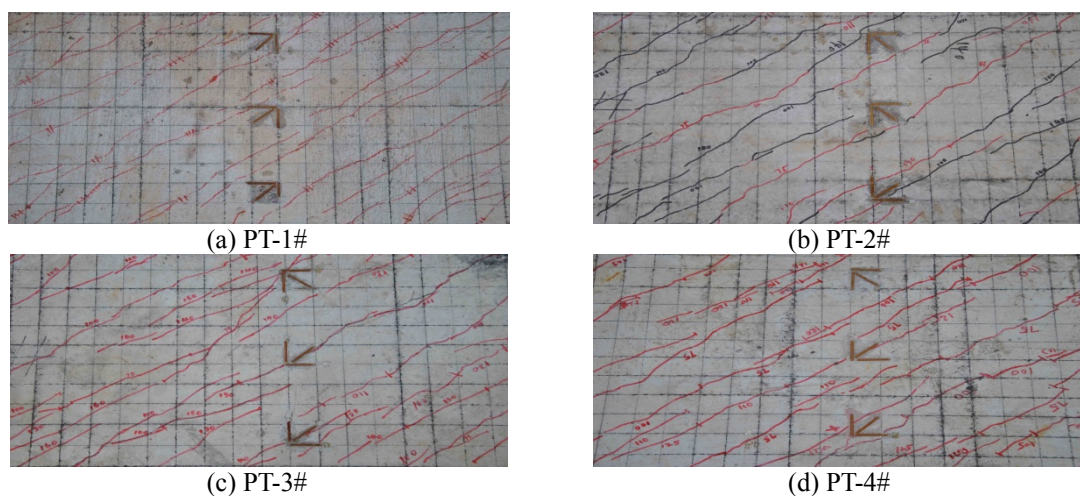

(a) PT-1#　　　　　　　　　　　　　　　　(b) PT-2#

(c) PT-3#　　　　　　　　　　　　　　　　(d) PT-4#

Fig. 5 Final forms of diagonal cracks in the test area of the top slab

(a) 113.46 kN-m   (b) 150.51 kN-m   (c) 164.05 kN-m   (d) 179.13 kN-m

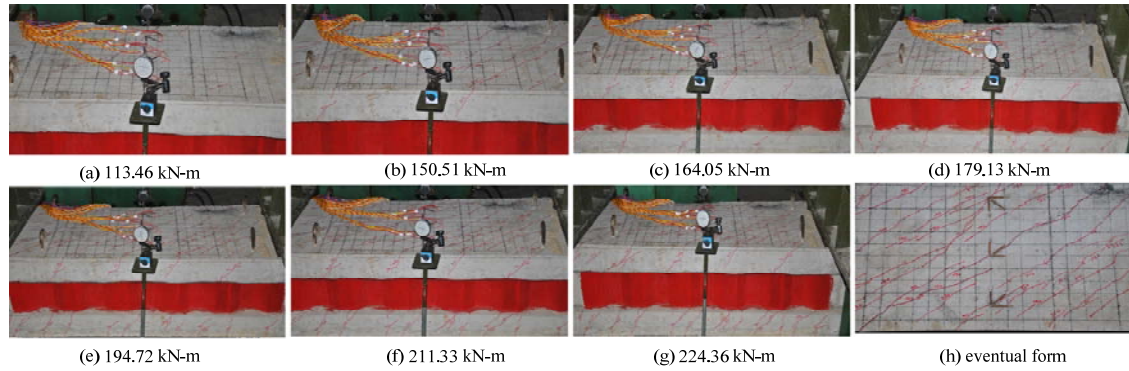(e) 194.72 kN-m   (f) 211.33 kN-m   (g) 224.36 kN-m   (h) eventual form

Fig. 6 The development of cracks in PT-3#

Table 3 Geometric and material parameters of specimens

Specimens	Cracking state		Yield state		Limit state		Failure mode
	T (kN-m)	*θ* (deg./m)	*T* (kN-m)	*θ* (deg./m)	*T* (kN-m)	*θ* (deg./m)	
PT-1	113.63	0.228	191.14	1.314	200.00	1.643	Shear failure
PT-2	115.60	0.269	196.61	1.059	222.67	1.846	Shear failure
PT-3	113.46	0.100	164.05	0.250	224.36	1.155	Shear failure
PT-4	113.20	0.192	113.20	0.192	180.92	1.069	Shear failure

4.2 Torsional bearing capacity

Table 3 lists the value of torque and twist of specimens in the state of cracking, yield of corrugated steel webs and ultimate limit, respectively. It is not hard to observe that the ratios of cracking torque to ultimate torque are 56.8%, 51.9%, 50.6% and 62.6%, while those of yielding torque to ultimate torque are 95.6%, 88.1%, 73.1% and 62.6% individually. It indicates that the thickness of corrugated steel webs has little effect on cracking torque but affects yielding torque considerably. The ratio of yielding torque to ultimate torque becomes higher as the thickness of corrugated steel webs increases.

The torque-twist relationship of each of all four specimens, which was obtained from the test, is shown in Fig. 7, in which the three stages mentioned above are clearly presented. Before cracking, the torque and twist are found to have a linear relationship and the slope of the curve is the torsional rigidity of composite box girder. The tangent slope of torque-twist curve of each of all four specimens decreases after cracking which indicates the torsional rigidity decreases simultaneously.

4.3 Shear strain of corrugated steel webs

Fig. 8 shows the relation curves between torque and shear strain of corrugated steel webs. The shear strain of corrugated steel webs is linearly proportional to external torque before steel webs yield, while that is nonlinear after yielding. It can be seen from Fig. 8 that steel webs yield when the composite box girder approaches its ultimate bearing capacity in PT-1 and PT-2 specimens, and
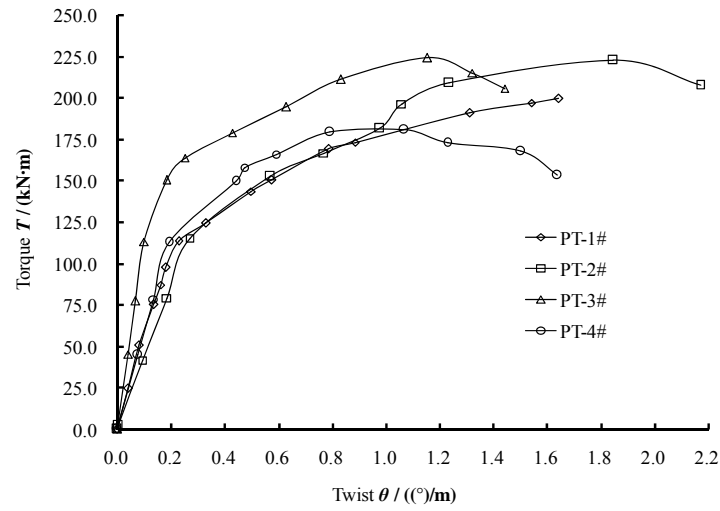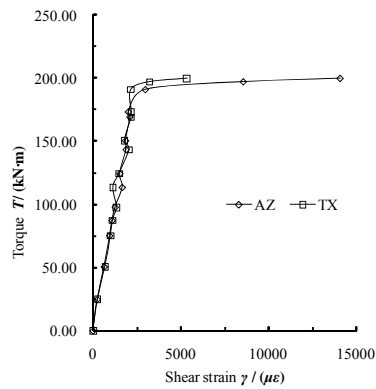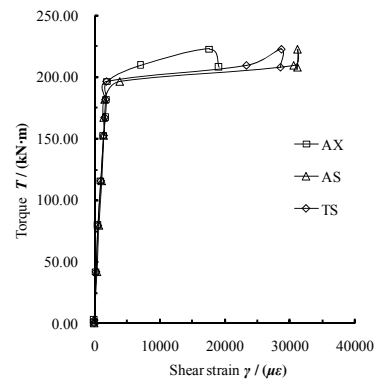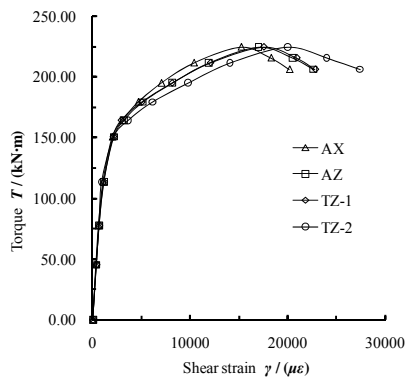
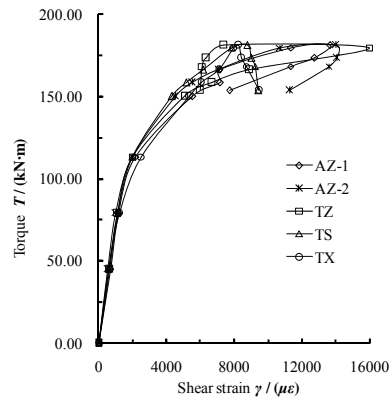Fig. 7 Torque-twist relationships of all four specimens

(a) PT-1#

(b) PT-2#

(c) PT-3#

(d) PT-4#

Fig. 8 Shear strain-torque relationship of all four specimens
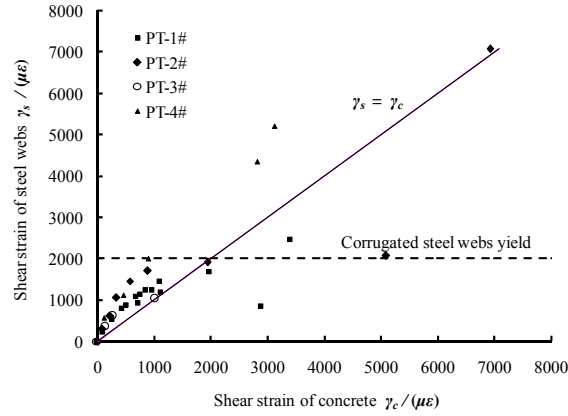
Fig. 9 Comparison of shear strain between top slabs and steel webs

that those yield before the ultimate bearing capacity in PT-3 and PT-4 specimens. It can be explained by the difference in thickness of steel webs of all four specimens. When the steel webs are in yield state, shear flow q resisted by thicker steel webs is larger than that resisted by thinner ones, which is equal to yield stress τy multiplied by thickness of steel webs tw. It also indicates that external torque can be resisted by the top and bottom concrete slabs continuously after the yield of thinner corrugated steel webs.

There is a debate on shear strain between concrete slabs and corrugated steel webs (Mo 2000 and Nie 2007). To obtain a full understanding of torsional behavior of CBCSWs and to lay an experimental foundation for theoretical analysis, the shear strain of corrugated steel webs and concrete slabs of all four specimens are compared as shown in Fig. 9. The x-coordinate denotes the shear strain of concrete slabs γc, and y-coordinate the shear strain of corrugated steel webs γs. It can be observed from Fig. 9 that the shear strain of corrugated steel webs is larger than that of the top concrete slab before the corrugated steel webs yield and the data is discrete for little samples after yielding. This indicates the hypothesis that the shear strain of corrugated steel webs is equal to that of concrete slabs before the corrugated steel webs yield, is not reasonable.

4.4 Strain of longitudinal reinforcement and stirrup

Fig. 10 ~ Fig. 13 show the relation curves between torque and strain of longitudinal reinforcement and stirrups of all four specimens. The first character in the gauge designation, such as *T*, or *B*, represents the location of rebar in top slab or in bottom slab. The second character *O* or *I* stand for outer surface or inner surface. The third character *T* or *L* denotes on stirrups or on longitudinal reinforcement and Arabic numerals such as 1, 2, or 3 represents the number of strain gauge. For example, TIT-1 means the first gauge which is located on stirrup in inner surface of top slab.

As shown in Fig. 10 ~ Fig. 13, the strain of stirrups and longitudinal reinforcement is linearly proportional to external torque at the beginning of loading. Subsequently, the strain of rebar increases considerably as the torque increases and the relationship is nonlinear. This is because when the external torque exceeds cracking torque, cracks appear in the concrete, which results in the transfer oftensile stress from the concrete to the rebar. It can also be observed that the strain of rebar located in the outer surface is larger than that in the inner surface at the same external torque,
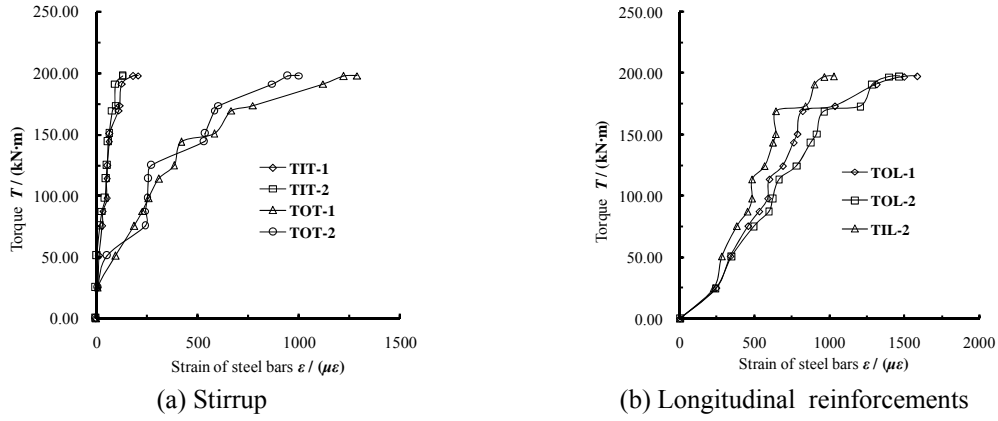
Yong Ding, Kebin Jiang, Fei Shao and Anzhong Deng

(a) Stirrup   (b) Longitudinal reinforcements

Fig. 10 Strain-torque relationship of PT-1#

(a) Stirrup   (b) Longitudinal reinforcements
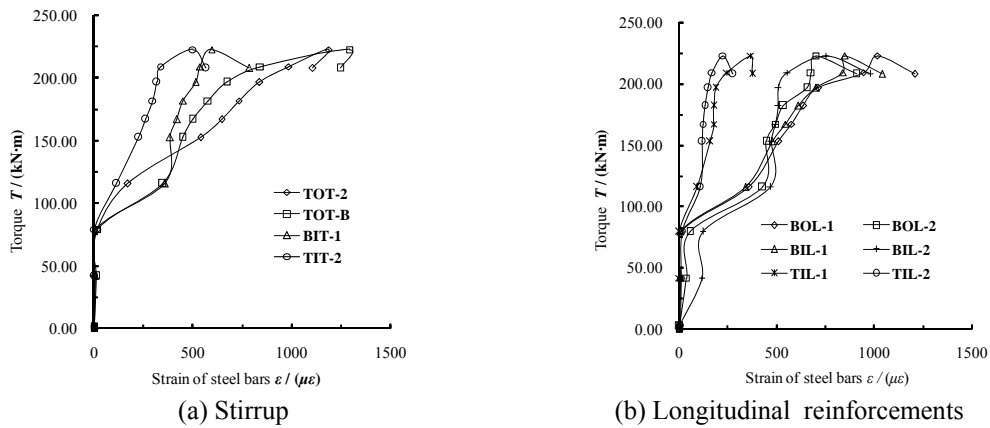
Fig. 11 Strain-torque relationship of PT-2#

(a) Stirrup   (b) Longitudinal reinforcements
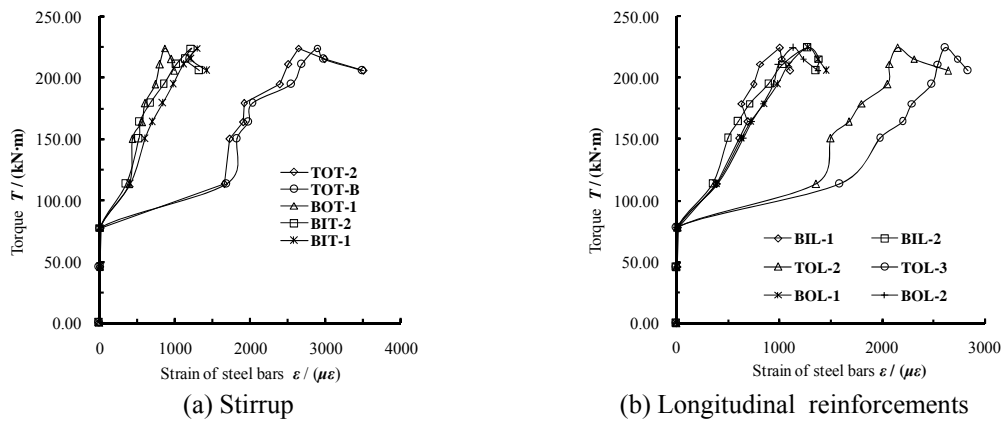
Fig. 12 Strain-torque relationship of PT-3#
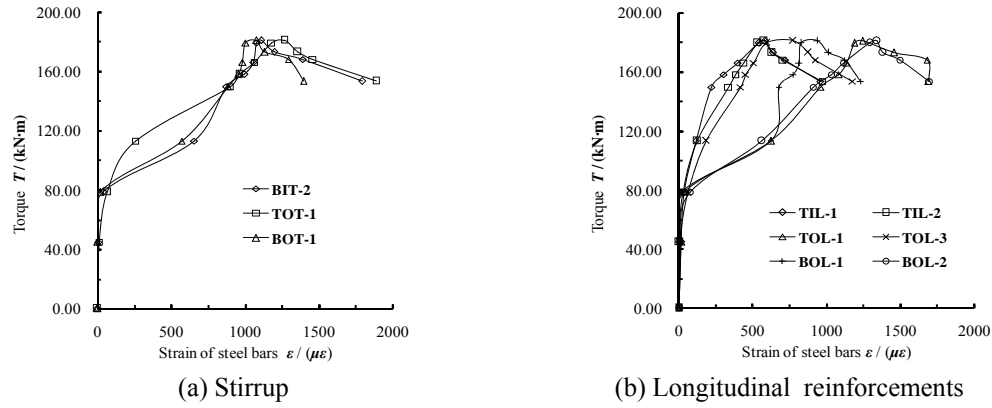
(a) Stirrup

(b) Longitudinal reinforcements

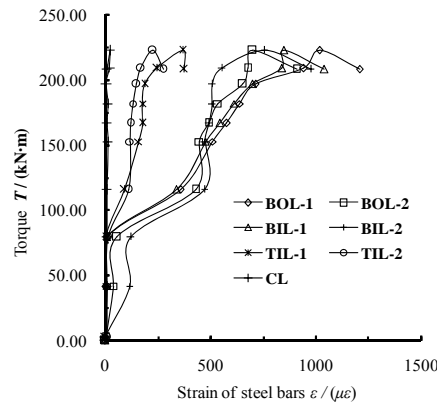Fig. 13 Strain-torque relationship of PT-4#

Fig. 14 Strain of longitudinal reinforcement located in different areas of PT-2#

which indicates that shear flow zone develops from the outer surface into the inner surface during the whole process of loading.

4.5 Strain of rebar located in sectional center

Fig. 14 gives a comparison of strain of longitudinal rebar located in the top, bottom concrete slab and the middle of the section. As external torque increases, strain of longitudinal rebar located in the outer surface of the top and bottom concrete slabs increases the most, followed by that located in the inner surface, but the strain of longitudinal rebar located in the middle of the section is very small and keeps invariant during the whole process of loading. Therefore a conclusion can be safely drawn that rebar which is located in the middle of section makes minor contribution to resisting external torque.

4.6 Effection of corrugation shape

Corrugation shape is of no effect on torsional bearing capacity but of much on torsional rigidity

of CBCSWs as can be concluded from Table 3. The value of shape parameter η corresponding to different corrugation shapes is various. For equivalent shear modulus G_e is equal to ηG, in which G means shear modulus of steel plate. As a result, larger η induces larger G_e which results in larger torsional rigidity of CBCSWs. It is clearly shown in Fig. 7 that the torsional rigidity of PT-3 with corrugation shape of CII, which has a larger value of η as listed in Table 1, is larger than that of the other three specimens with corrugation shape of CI.

4.7 Effection of thickness of steel webs

From Table 3, it can be obtained that yielding torque and ultimate torque are proportional to thickness of steel webs, that is to say, yielding torque and ultimate torque increase as the thickness increases. As shown in Fig. 7 and Table 3, it can be concluded that thickness of steel webs influences yielding torque and ultimate torque greatly but has little effect on torsional rigidity of CBCSWs. This is because the thickness of steel webs is relatively small compared to that of the top and bottom concrete slabs. Consequently, the torsional rigidity of CBCSWs is insensitive to thickness variation of steel webs.

5. Conclusions

Through the model test of four PC composite box-girders with corrugated steel webs under monotonic pure torsion, conclusions can be drawn as follows:
• All diagonal cracks in the surface of concrete slabs are inclined at an angle of approximately 45° to the specimen's longitudinal axis, and the loss of torsional bearing capacity of all four specimens is under the control of primary cracking, not secondary one.
• In the case of thin steel webs, the PC composite box-girders with corrugated steel web can resist external torque by the top and bottom concrete slabs continually after steel webs yield. The thinner the steel webs are, the smaller the ratio of yielding torque to ultimate torque is.
• It is not reasonable to adopt the assumption in theoretical analysis that the shear strain of corrugated steel webs is equal to that of concrete slabs, for larger shear strain of steel webs compared with concrete slabs is observed in the model test. The experimental phenomenon that the strain of rebar located in the outer surface is larger than that of rebar located in the inner surface during the whole process of loading is consistent with the view that shear flow zone develops from the outer surface into the inner surface.
• Longitudinal reinforcement located in the center of cross section contributes little to torsional bearing capacity of the specimens and corrugation shape has great effect on torsional rigidity. The specimen with larger shape parameter η has higher torsional rigidity.
• The thickness of steel webs influences yielding torque and ultimate torque greatly based on experimental observation. Yielding torque and ultimate torque decrease as the thickness of steel webs decreases.

Acknowledgments

conclusions of the paper are the authors' and do not necessarily represent the views of the sponsors.

References

Cheyrezy, M. and Combault, J. (1990), "Composite bridges with corrugated steel webs-achievements and prospects", *IABSE Symposium on Mixed Structures Including New Materials*, Brussels.

Metwally, A.E. and Loov, R.E. (2003), "Corrugated steel webs for prestressed concrete girders", *Materials and Structures*, **36**, 127-134.

Combault, J. (1988), "The Maupre Viaduct near Charolles", *France Proceeding of 1988 National Steel Construction Conference*, (6).

Elgaaly, M., Seshadri, A. and Hamilton, R.W. (1997), "Bending strength of steel beams with corrugated webs", *Journal of Structural Engineering*, **123**(6), 772-782.

Elgaaly, M. and Seshadri, A. (1998), "Depicting the behavior of girders with corrugated webs up to failure using nonlinear finite element analysis", *Advances in Engineering Software*, **29**(3-6), 195-208.

Moon, J.H., Yi, J.W. and Choi, B.H. *et al.* (2009), "Shear strength and design of Trapezoidally corrugated steel webs", *Journal of Constructional Research*, **65**, 1198-1205.

Yi, J.W., Gil, H.B. and Youm, K.S. *et al.* (2008), "Interactive shear buckling behavior of Trapezoidally corrugated steel webs", *Engineering Structure*, **30**, 1659-1666.

Elgaaly, M. and Hamilton, R.W. (1996), "Shear strength of beam with corrugated webs", *Journal of Structural Engineering*, **122**(4), 390-398.

Song, J.Y., Zhang, S. and Wang, T. *et al.* (2004), "A theoretical analysis and experimental study on the flexural behavior of externally prestressed composite beam with corrugated steel webs", *China Civil Engineering Journal*, **37**(11), 50-55. (in Chinese)

Jiang, K., Ding, Y. and Liu, Y. *et al.* (2011), "Analysis on secondary effect of corrugated webs in steel-concrete composite beams", *Advanced Materials Research*, **255-260,** 596-601.

Chuslip, P. and Usami, T. (2002), "Strength and ductility of steel box girders under cyclic shear", *Journal of Structural Engineering*, **128**(9), 1130-1138.

Driver, R.G., Abbas, H.H. andd Sause, R. (2006), "Shear behavior of corrugated web bridge girders", *Journal of Structural Engineering*, 132(2), 195-203.

Cevik, A., Arslan, M.H. and Saracoglu, R. (2012), "Neuro-fuzzy modeling of torsional strength of RC beams", *Computers and Concrete*, **9**(6), 469-486.

Mo, Y.L., Jeng, C.H. and Chang, Y.S. (2000), "Torsional behavior of prestressed concrete box-girder bridges with corrugated steel webs", *ACI Structural Journal*, **97**(6), 849-859.

Ding, Y., Jiang, K. and Liu, W. (2012), "Nonlinear analysis for PC box-girder with corrugated steel webs under pure torsion", *Thin-walled Structures*, **51**, 167-173.

European Committee for Standardization (CEN) (2005), Eurocode 3: Design of steel structures, part 1-8: design of joints (EN 1993-1-8:2005), Brussels.

American Institute of Steel Construction (AISC) (2005), Specification for structural steel buildings, ANSI/AISC 360-05, Chicago (IL).

Ministry of Communications P.R.China (2004), JTG D62-2004 Code for design of highway reinforced concrete and prestressed concrete bridges and culverts, Beijing: China Communications Press, 1-236. (in Chinese)

Nie, J.G. and Tang, L. (2007), "Nonlinear analysis of pure torsion property for prestressed concrete composite box girder with corrugated steel webs", *China Journal of Highway and Transport*, **20**(5), 71-77. (in Chinsese)